CONTROL LAWS FOR AN AIRCRAFT SUPERSONIC INLET WITH MOBILE PANEL

Alexandru Nicolae TUDOSIE

University of Craiova, Craiova, Romania (atudosie@elth.ucv.ro)

DOI: 10.19062/2247-3173.2017.19.1.26

Abstract: *The paper studies a rectangular supersonic inlet for a 2.5 Mach aircraft. Inlet's architecture was chosen in order to assure a wide range of flight regimes (from low regimes of taxi and take-off until high supersonic regime), so it was built with a mobile panel. Applying an algorithm based on inlet's efficiency maximization, the optimal architecture for the most employed flight regime was determined and inlet's characteristics maps for a fixed geometrical configuration were obtained. In order to obtain the flow characteristics improvement, an adjusting law for the mobile panel was imagined and, consequently, some new characteristics maps issued; a complementary law was also described and established. The study is useful for further inlet's automation possibilities analysis and also for combined control law(s) issuing, as well as for similar inlets architecture establishing.*

Keywords: *inlet, control law, ramp, cowl, shock-wave, pressure, supersonic.*

1. INTRODUCTION

Most modern passenger and military aircraft are powered by gas turbine engines (jet engines, turboprops, turbofans, propfans), but several are powered by ramjets. There are lot of different types of aircraft engines, but all these have some parts in common. All engines should have an inlet to bring the air stream inside the engine. For the gas turbine engines, the inlet sits upstream of the compressor and, while the inlet does no work on the flow, there are some important design features of the inlet.

Inlets come in a variety of shapes and sizes with the specifics usually dictated by the speed of the aircraft. Engine's inlet is required to provide the proper quantity and uniformity of air to the engine over a wide range of flight conditions (altitudes and speeds). For aircraft that cannot fly faster than the speed of sound (such as large airliners), inlets' shapes are simple, so a straight, short and low profiled inlet works quite well. A subsonic aircraft has an inlet with a relatively thick lip.

On the other hand, for a supersonic aircraft, the inlet must slow the flow down to subsonic speeds before the air reaches the compressor. An inlet for a supersonic aircraft has a relatively sharp lip. This lip is sharpened to minimize the performance losses from shock waves that occur during supersonic flight. Some supersonic axis-symmetrical inlets use central cones (conical-shaped centerbodies). Other inlets use flat hinged plates or a spike-shaped centerbodies (plan-parallel inlets with rectangular cross section) to shock the flow down to subsonic speeds and to generate the compression through these shock-waves; this kind of inlet is seen on the F-14 and F-15 or on the Mig-29 fighter aircraft. There are other, more exotic inlet shapes used on some aircraft for a variety of reasons.

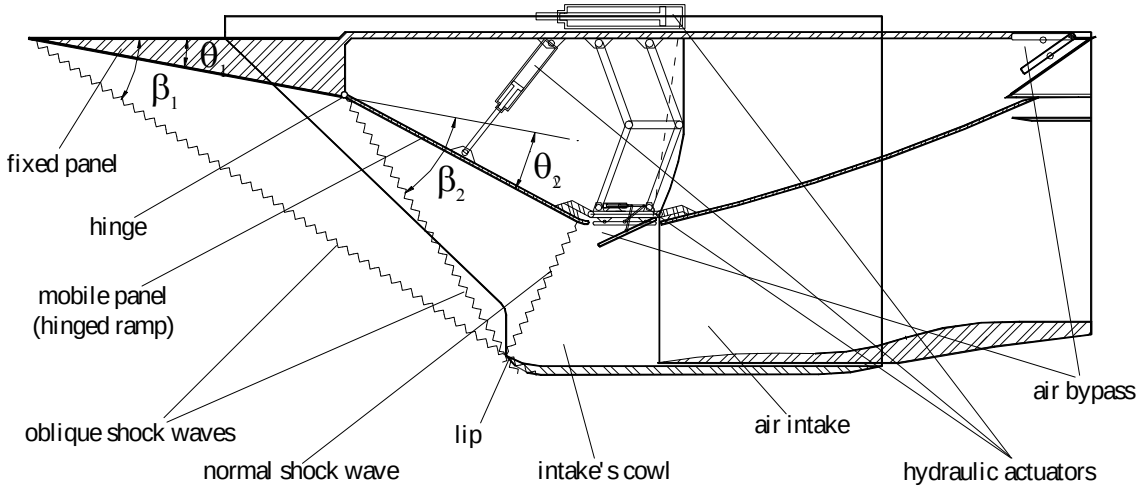

FIG. 1. Supersonic inlet with mobile panel "2+1"-type [12]

An inlet, no matter its architecture, must operate efficiently over the entire flight envelope of the aircraft. At very low aircraft speeds, or when just sitting on the runway, free stream air is "sucked" into the engine by the compressor. Meanwhile, at high speeds, an appropriate designed and manufactured inlet will allow the aircraft to maneuver to high angles of attack and sideslip, without disrupting the air flow to the compressor. It is well known that a loss of 1% from intake's total air pressure will lead to 0.5÷1.2 % lowering of engine's thrust, as stated in [4, 6, 9].

Because the inlet is so important to overall aircraft operation, it is usually designed and tested by the airframe company, not by the engine manufacturer; that is the reason because all engine manufacturers also employ aerodynamic engineers for inlet design.

The paper studies a plan supersonic inlet with a single mobile ramp, operating on a supersonic M_H=2.5 aircraft, mounted below its wing, as the one in Fig.1.

2. INLET ARCHITECTURE

The inlet in Fig. 1 consists of an air intake (which could have a fixed or a mobile cowl) and a spike-shape body with two different plates (a fixed panel and a hinged panel), assisted by hydraulic actuators. The inlet is mounted below aircraft's wing; consequently, in supersonic flight, air speed in front of the air intake is less than the airspeed of the airplane, because of two shock waves: the first one is conical and it is triggered by aircraft's nose, the second one – by aircraft's wing. Meanwhile, during supersonic operating, the inlet has its own shock wave system, generated by the spike and by cowl's lip: two oblique shock-waves due to spike's panels and a final normal shock wave attached to the cowl's lip.

Mobile panel could have three different positions, as follows: a) for subsonic flights it is completely retracted ($\theta_2 < 0$), offering to the intake the maximum air-breathing cross-section; b) for moderate supersonic flights, the mobile panel is on the fixed one's direction ($\theta_2 = 0$), extending it; c) for high supersonic flights the mobile panel has variable position ($\theta_2 > 0$, as Fig. 1 shows), according to the air velocity in front of the inlet.

Inlet's characteristics are: a) the efficiency characteristic (inlet's total pressure loss σ_i^* versus inlet's front Mach number) and b) the flow characteristic (inlet's flow ratio coefficient C_D versus inlet's front Mach number).

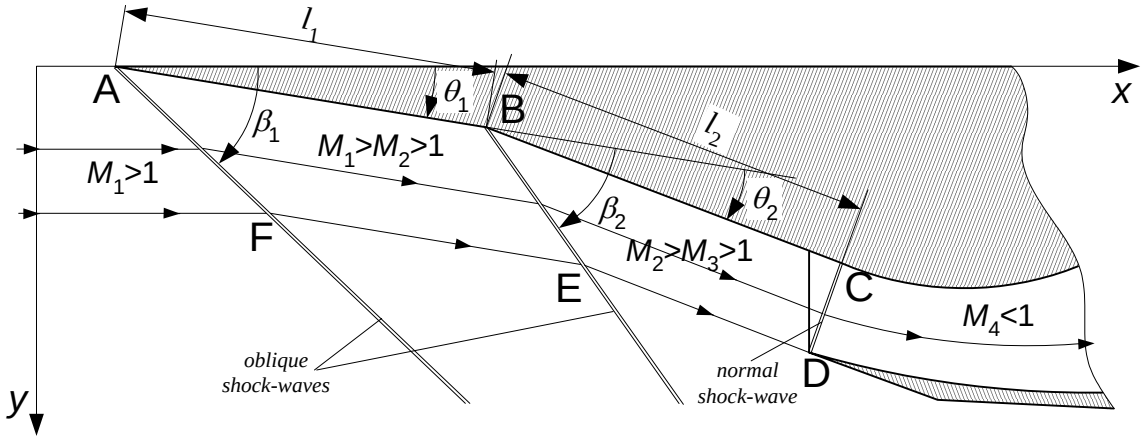

FIG. 2. Supersonic inlet "2+1"-type geometry

Some particular inlets with mobile panels have even the possibility of intake's blocking, by completely mobile panel's pull out until it reaches the cowl [10]; this regime characterizes the ground operating (engine's ground test, aircraft ground maneuvering, low speed take-off running etc.), when the engine's air breathing is realized through a system of upper flaps, which are automatically open simultaneously with the main intake's close; main reason for this behavior are connected to engine's protection against accidental suction into the turbo-engine of small objects on the runway, or on the test platform.

This kind of inlet assures a wide range of aircraft flight regimes (flight altitudes and speeds), as well as the whole range of engine's operating engines.

For an aircraft designed to reach a flight Mach number of 2.5, air velocity in front of this kind of inlet corresponds to a Mach number of 2.1, because of successive shock down of the air flow through the shock-waves triggered by aircraft's aerodynamic shape.

3. OPTIMAL INLET CONFIGURATION

Inlet design is an important engineering issue, involving geometric, aerodynamic and energetic grounds. Design methods and algorithms are presented in [6,7,10], different optimization criteria being emphasized.

An algorithm of geometric optimization of an external compression inlet, such as the one in fig. 2 is presented in [7] and is based on inlet's efficiency maximization. This algorithm aims to determine optimum values of spike's angles θ_1 and θ_2, as well as a dimensionless geometry of the inlet; it was also applied for the optimization of the rectangular inlet studied in [12].

Performance criterion for optimization is the maximum inlet efficiency, or else, maximum inlet total pressure loss (or recovery) co-efficient σ_i^*, given by

$$\sigma_i^* = \sigma_{osw1}^* \sigma_{osw2}^* \sigma_{nsw}^* \sigma_d^*, \tag{1}$$

where σ_{osw1}^*, σ_{osw2}^* are total pressure ratios for the oblique shock-waves, σ_{nsw}^* – total pressure ratio for the normal shock-wave and σ_d^* – total pressure ratio into intake's duct (assumed as constant, no matter the flight regime or the engine regime would be).

Each term in Eq. (1) is given by the aerodynamic and thermodynamic conditions of shock waves, as follows:

- for the oblique shock waves

$$\sin^2\beta_k = \frac{1}{M_k^2} + \frac{\chi+1}{2}\frac{\sin\beta_k \cdot \sin\theta_k}{\cos(\beta_k - \theta_k)}, \tag{2}$$

$$M_{k_{av}}^2 = \frac{1}{\sin^2(\beta_k - \theta_k)}\frac{(\chi-1)M_k^2\sin^2\beta_k + 2}{2\chi M_k^2\sin^2\beta_k - (\chi-1)}, \tag{3}$$

$$\sigma_{oswk}^* = \left[\frac{(\chi+1)M_k^2\sin^2\theta_k}{2+(\chi-1)M_k^2\sin^2\theta_k}\right]^{\frac{\chi}{\chi-1}}\left[\frac{\chi+1}{2\chi M_k^2\sin^2\theta_k - (\chi-1)}\right]^{\frac{1}{\chi-1}}, \tag{4}$$

where $k = \overline{1,2}$, M_k – Mach number before the shock-wave, $M_{k_{av}}$ – Mach number behind the shock-wave;

- for the normal shock-wave

$$M_{av}^2 = \frac{(\chi-1)M_k^2 + 2}{2\chi M_k^2 - (\chi-1)}, \tag{5}$$

$$\sigma_{nsw}^* = \left[\frac{(\chi+1)M_k^2}{2+(\chi-1)M_k^2}\right]^{\frac{\chi}{\chi-1}}\left[\frac{\chi+1}{2\chi M_k^2 - (\chi-1)}\right]^{\frac{1}{\chi-1}}, \tag{6}$$

where M_k – Mach number before the shock-wave, M_{av} – Mach number behind the shock-wave, χ – air's adiabatic exponent.

First inlet configuration design issue is the determination of the spike's angles values, starting from the nominal Mach number value in front of the inlet.

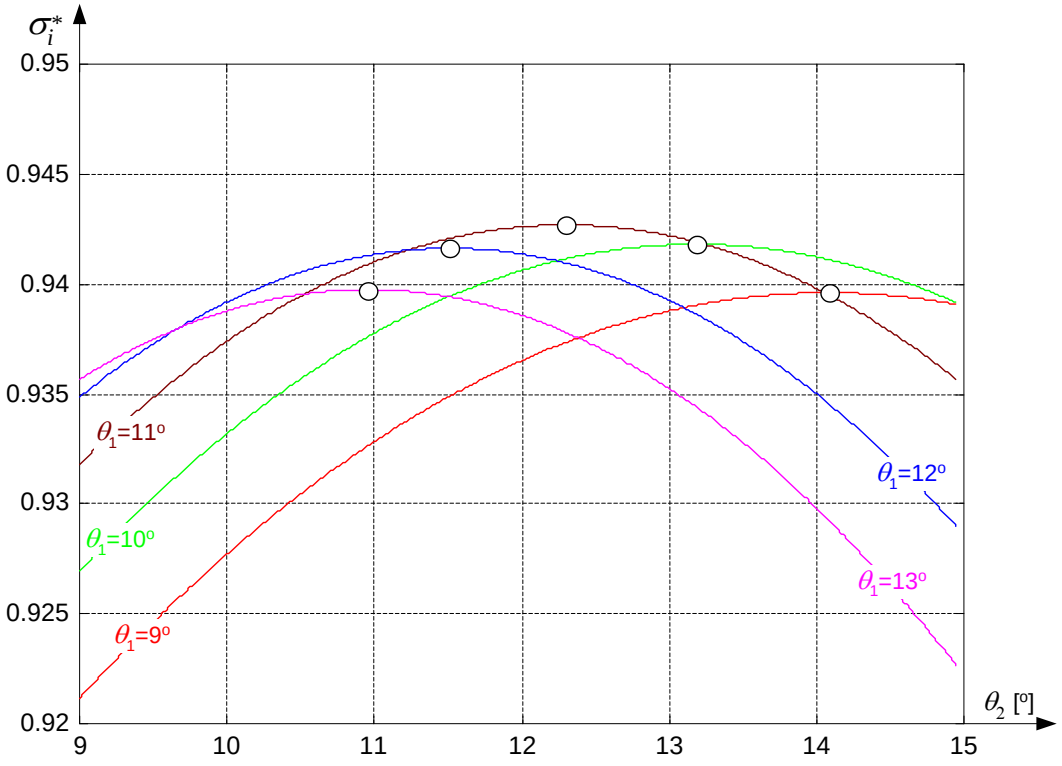

FIG. 3. Total pressure recovery co-efficient versus second panel's angle, for different values for first panel's angle

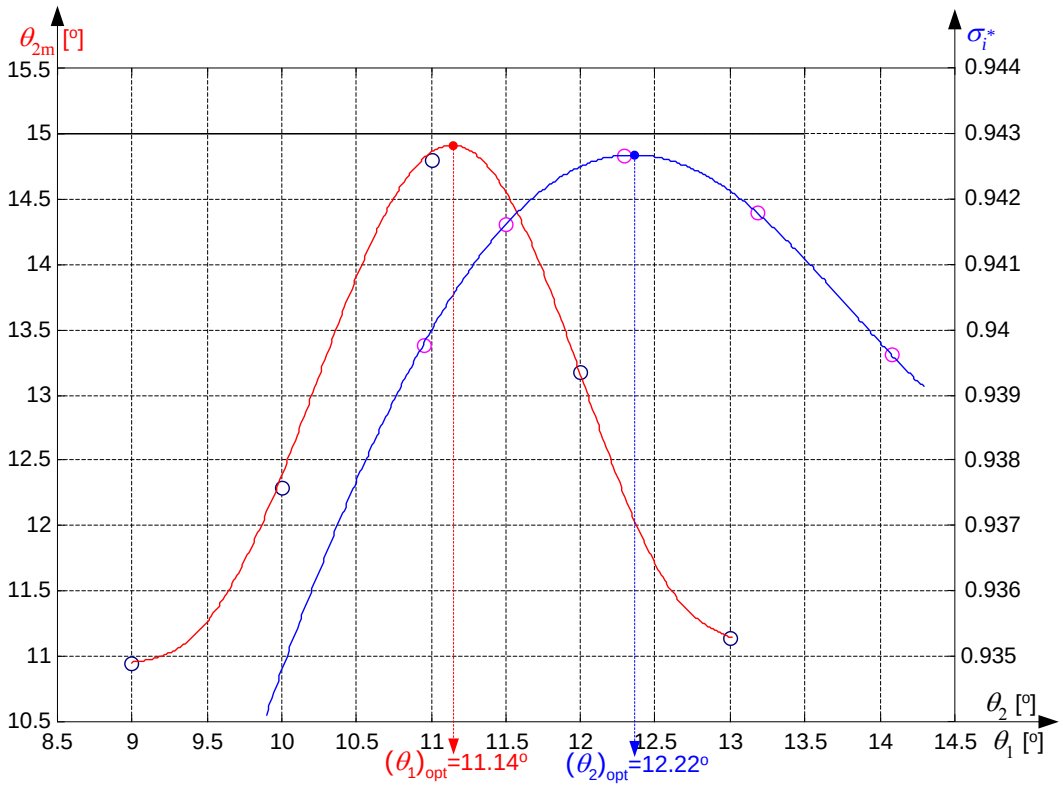

FIG. 4. Panels' angles optimal values determination

For a flight Mach number $M_H = 2.5$, inlet front value M_1 should be around 2.1; starting from this value, one can apply the algorithm, in order to obtain the maximization of σ_i^*. One has to choose intervals of values for θ_1 and for θ_2 and, applying Eqs. (2)…(6), one obtains values for σ_i^*, in fact a family of curves $\sigma_i^* = \sigma_i^*(\theta_2)_{\theta_1}$, as Fig. 3 shows.

Each curve in Fig. 3 has a maximum value point, which correspond to the optimal value of θ_2 -parameter, so one can build the graph $\theta_{2_{opt}} = \theta_{2_{opt}}(\theta_1)$; as Fig. 4 shows, the maximum value of the curve correspond to the optimal value of θ_1. Consequently, one has obtain both optimal values $\theta_{1_{opt}}$ and $\theta_{2_{opt}}$, which give the maximum value of σ_i^*.

Optimal inlet geometry should be obtained considering the situation when both oblique shock-waves are attached to the cowl's lip (see Fig.1), or shock focal point is situated on cowl's lip. Considering that cowl's lip point D represents the unitary coordinate $(y_D = 1)$, one can determine inlet's dimensionless geometry. With these optimal values of spike's angles one obtains the co-ordinates for the characteristic points in Fig. 2, as follows

$$\begin{aligned} &A(0;0),\ B\left(l_1\cos\theta_{1_{opt}};l_1\sin\theta_{1_{opt}}\right),\ D\left(\frac{1}{\mathrm{tg}\beta_1\left(\theta_{1_{opt}}\right)};1\right), \\ &C\left(l_1\cos\theta_{1_{opt}}+l_2\cos\left(\theta_{1_{opt}}+\theta_{2_{opt}}\right);l_1\sin\theta_{1_{opt}}+l_2\sin\left(\theta_{1_{opt}}+\theta_{2_{opt}}\right)\right). \end{aligned} \tag{7}$$

where the lengths l_1 and l_2 of the spike panels in Fig. 2 are

$$l_1 = \frac{\mathrm{tg}\beta_1\left(\theta_{1_{\mathrm{opt}}}\right) - \mathrm{tg}\left[\theta_{1_{\mathrm{opt}}} + \beta_2\left(\theta_{2_{\mathrm{opt}}}\right)\right]}{\cos\theta_{1_{\mathrm{opt}}}\,\mathrm{tg}\beta_1\left(\theta_{1_{\mathrm{opt}}}\right)\left\{\mathrm{tg}\theta_{1_{\mathrm{opt}}} - \mathrm{tg}\left[\theta_{1_{\mathrm{opt}}} + \beta_2\left(\theta_{2_{\mathrm{opt}}}\right)\right]\right\}}, \tag{8}$$

$$l_2 = \frac{1}{\cos\left(\theta_{1_{\mathrm{opt}}} + \theta_{2_{\mathrm{opt}}}\right)\mathrm{tg}\beta_1\left(\theta_{1_{\mathrm{opt}}}\right)\left[1 + \mathrm{tg}^2\left(\theta_{1_{\mathrm{opt}}} + \theta_{2_{\mathrm{opt}}}\right)\right]}\left\{1 + \mathrm{tg}\left(\theta_{1_{\mathrm{opt}}} + \theta_{2_{\mathrm{opt}}}\right)\mathrm{tg}\beta_1\left(\theta_{1_{\mathrm{opt}}}\right) - \right.$$

$$\left. - \frac{\mathrm{tg}\beta_1\left(\theta_{1_{\mathrm{opt}}}\right) - \mathrm{tg}\left[\theta_{1_{\mathrm{opt}}} + \beta_2\left(\theta_{1_{\mathrm{opt}}}\right)\right]}{\mathrm{tg}\theta_{1_{\mathrm{opt}}} - \mathrm{tg}\left[\theta_{1_{\mathrm{opt}}} + \beta_2\left(\theta_{1_{\mathrm{opt}}}\right)\right]}\left[\mathrm{tg}\theta_{1_{\mathrm{opt}}}\,\mathrm{tg}\left(\theta_{1_{\mathrm{opt}}} + \theta_{2_{\mathrm{opt}}}\right) + 1\right]\right\}. \tag{9}$$

For a Mach number in front of the inlet $M_1 = M_{1_{\mathrm{nom}}} = 2.1$, one has obtained, for a fixed geometry inlet, the results: $\theta_{1_{\mathrm{opt}}} = 11.14^\circ$, $\theta_{2_{\mathrm{opt}}} = 12.22^\circ$, $l_1 = 0.8849$, $l_2 = 0.7624$ and the coordinates of the characteristic points are A (0,0); B (0.874; 0.142); C (1.569; 0.454); D (1.324; 1).

For different M_1 Mach numbers, lower than the design Mach number ($M_1^{/} < M_{1_{\mathrm{nom}}}$), but for fixed inlet geometry, oblique shock-waves are depleting, see Fig. 3, so angles β_1 and β_2 are growing, which means that σ_i^* and C_D are modifying too. While σ_i^* can be calculated with above-mentioned formulas ((1), (4) and (6)), C_D is represented by the inlet's effective air-breathing area $A_H / A_{1^{/}}$, which is exactly the co-ordinate y_F in Fig. 3:

$$C_D = \frac{A_H}{A_{1^{/}}} = \frac{A_H}{(A_H)_{\mathrm{nom}}} = \frac{b \times y_{\mathrm{F}}}{b \times y_{\mathrm{D}}} = \frac{y_{\mathrm{F}}}{y_{\mathrm{D}}} = y_{\mathrm{F}}, \tag{10}$$

E-point and F-point coordinates are:

$$x_{\mathrm{E}} = \frac{y_{\mathrm{B}} - y_{\mathrm{D}} + x_{\mathrm{D}}\mathrm{tg}\left(\theta_{1_{\mathrm{opt}}} + \theta_{2_{\mathrm{opt}}}\right) - x_{\mathrm{B}}\mathrm{tg}\left(\theta_{1_{\mathrm{opt}}} + \beta_2^{/}\right)}{\mathrm{tg}\left(\theta_{1_{\mathrm{opt}}} + \theta_{2_{\mathrm{opt}}}\right) - \mathrm{tg}\left(\theta_{1_{\mathrm{opt}}} + \beta_2^{/}\right)},$$

$$y_{\mathrm{E}} = y_{\mathrm{D}} + \left(x_{\mathrm{E}} - x_{\mathrm{D}}\right)\mathrm{tg}\left(\theta_{1_{\mathrm{opt}}} + \theta_{2_{\mathrm{opt}}}\right), \tag{11}$$

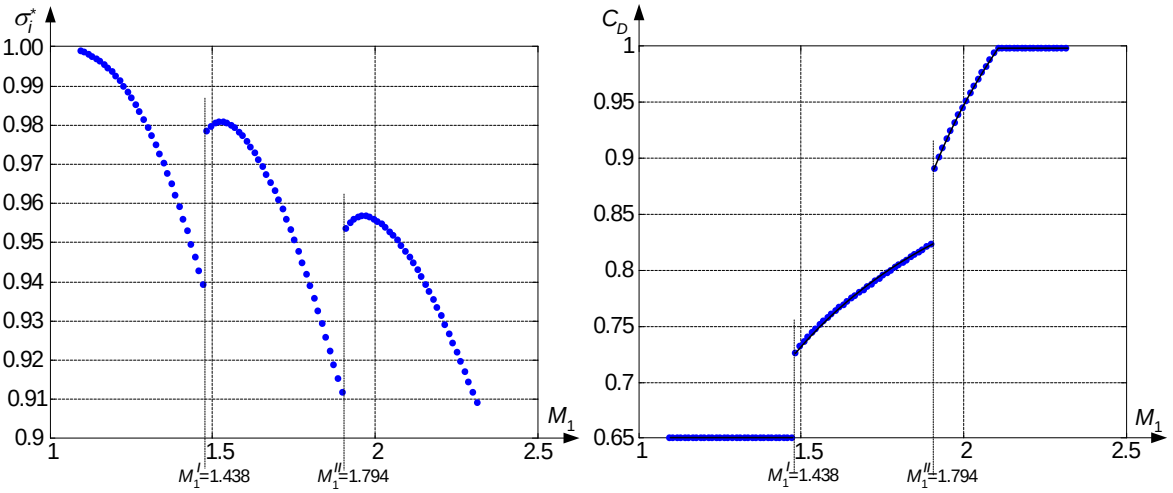

a) Inlet efficiency characteristic map b) Inlet flow rate characteristic map

FIG. 5. Inlet's characteristic maps (fixed geometry architecture)

$$x_F = \frac{y_E - x_E \operatorname{tg}\theta_{1_{opt}}}{\operatorname{tg}\beta_1' - \operatorname{tg}\theta_{1_{opt}}},\ y_F = x_F \operatorname{tg}\beta_1', \tag{12}$$

where values β_1' and β_2' are shock-wave's angle values calculated with respect to the new Mach number, but for the same spike angle values: $\beta_1' = \beta\left(M_1', \theta_{1_{opt}}\right)$, $\beta_2' = \beta\left(M_2', \theta_{2_{opt}}\right)$.

Inlet's characteristic curves are presented in Fig. 5. One can observe two discontinuities points, which corresponds to oblique shock-waves detaching: a) when $M_1 = 1.438$, which corresponds to a flight Mach number $M_H = 1.7$ and there is only one normal shock-wave in front of the inlet; b) when $M_1 = 1.794$, which corresponds to a flight Mach number $M_H = 2.15$, the spike's first panel generates a first oblique shock wave but the second shock wave is still detached. Only after this Mach number the second shock-wave becomes oblique and the shock-wave system is restored.

4. MOBILE PANEL MOTION LAW

Operation of an inlet with fixed geometry architecture means a lot of losses from air flow rate's point of view, as Fig. 5.b shows; especially for low or medium Mach numbers, flow coefficient C_D is far from the maximum value 1, and it could lead to buzz behavior of the inlet, especially when the engine's regime decreases. In order to grow the C_D-value, an appropriate

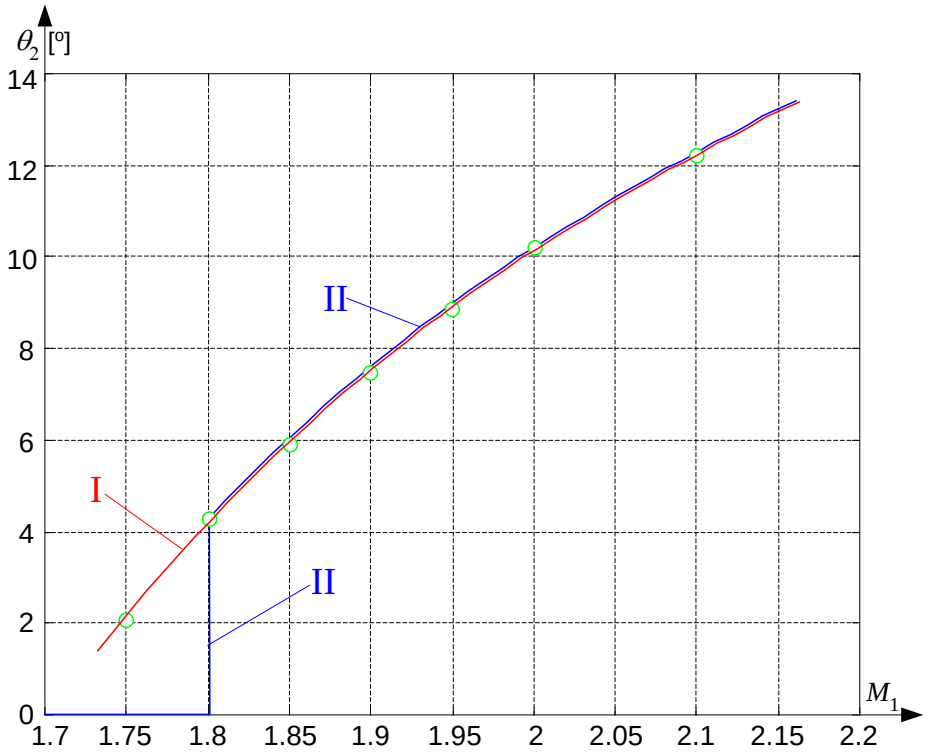

FIG. 6. Inlet's control law (mobile panel's angle versus Mach number in front of the inlet)

solution is to keep the second oblique shock-wave tangent (attached) to the cowl's lip, progressively growing the second spike angle θ_2, by rotating the mobile panel about its hinge. The condition of attaching the shock-wave is to keep constant the β_2 – angle, which means that one has to find the value of θ_2 which generates such an angle, with respect to the Mach number in front of the inlet; consequently, one has to solve the implicit equation where β_2 is the constant angle value, given by

the position of points B and D in Fig. 2, θ_2 – equation's argument, M_2 – Mach number behind the first oblique shock-wave and before the second oblique shock-wave, which is given by the value of Mach number in front of the inlet and the spike's first angle θ_1. Eventually, one obtains a dependence $\theta_2 = \theta_2(M_1)$, as curve I in Fig. 6 shows, which is a possible motion law for the mobile panel and a theoretical control law for the inlet.

$$\sin^2\beta_2 = \frac{1}{M_2^2} + \frac{\chi+1}{2}\frac{\sin\beta_2 \cdot \sin\theta_2}{\cos(\beta_2-\theta_2)}, \tag{13}$$

The curve in Fig. 6 is a bit non-linear, described by a polynomial expression as:

$$\theta_2(M_1) = 40.07 \cdot M_1^3 - 265.397 \cdot M_1^2 + 603.895 \cdot M_1 - 456.623\,[^\circ]. \tag{14}$$

It should be noted that even if the range of variation for θ_2 could begin at 0^o (which correspond to a theoretical Mach number $M_1 = 1.71$), because of second shock-wave's detachment under air speeds corresponding to $M_1 = 1.794$, it results that the domain of the control law must be restraint. Thus, the variation domain of θ_2 should begin at values bigger than $M_1^{//}$, which correspond to a minimum value $(\theta_2)_{\min} = 4.2^\circ$, so the aspect of the control law should be as the curve II in Fig. 6 shows. Moreover, aerodynamics studies have proved that small values for spike angles (under 4^o) didn't generate appropriate oblique shock-waves [6, 10], but detached normal shock-waves, supplementary reason for adopt the modified control law.

According to the above-presented issues, the inlet operates as "1+1" external compression device until the airspeed in front reaches a Mach number $M_1 = 1.8$, because the fixed panel and the mobile one are building a single-flare spike $\theta_2 = 0^\circ$ (see Fig. 7); at $M_1 = 1.8$ the mobile panel moves sudden at $(\theta_2)_{\min} = 4.2^\circ$, then, over this limit $M_1^b = 1.8$ Mach, the inlet behaves like a "2+1" external compression device, but with the second oblique shock-wave tangent to its

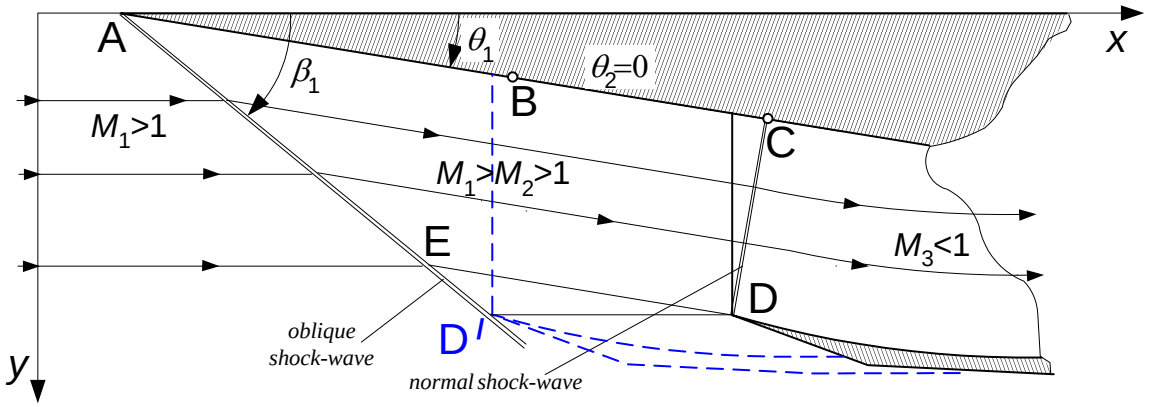

FIG. 7. Inlet's operation as "1+1" external compression device

cowl lip, until the nominal (design) flight Mach number value $(M_1)_{\text{nom}} = 2.1$ is reached.

Inlet's flow rate characteristics is improved, as shown in Fig. 9; curve I corresponds to inlet totally operation as "1+1" external compression device, while curve II is the flow rate characteristics of the inlet with mobile panel.

4. COMPLEMENTARY MOTION LAW (COWL DISPLACEMENT)

In spite of the above-mentioned improvement, inlet's behavior may be also improved for the "1+1" operation, from the flow rate characteristics point of view. Thus, in order to assure the maximum value of the flow coefficient C_D, the oblique shock-wave should be tangent to the cowl's lip, no matter the Mach number in front of the inlet. Since the spike has a fixed single flare, the only adjustment possibility remains intake's cowl displacement; therefore, a complementary law can be issued, which is intake's cowl positioning x_{ic} with respect to the Mach number in front of the inlet M_1.

According to Eq. (2) and as Fig. 7 shows, the oblique shock-wave's angle β_1 is given by the spike's angle θ_1 and the Mach number M_1, while D-point's co-ordinates are fixed, as determined in chapter 3 of the present paper. Consequently, cowl's displacement should reduce till cancellation the distance between the cowl's lip and the oblique the shock-wave, which means that D-point's new position must be D′ in Fig. 7; therefore, one has to determine the complementary law as:

$$x_{ic}(M_1) = x_{D'}(M_1) - x_D = \frac{1}{\mathrm{tg}\beta_1(\theta_1, M_1)} - 1.324\,. \tag{15}$$

From the intake's position point of view, when the Mach number in front of the inlet decreases, the cowl must be extended, so its extension should be equal to $|x_{ic}|$.

The front limit of the cowl's extension is reached for the Mach number M_1' (see Fig. 5), when the first oblique shock wave becomes detached; meanwhile, when M_1 becomes equal to $M_1^b = 1.8$ Mach, the main control law becomes active. Consequently, the domain of applying of this complementary law could be (M_1', M_1^b), as Fig. 8 shows.

An important observation should be made: if when the Mach number reaches M_1^b – value

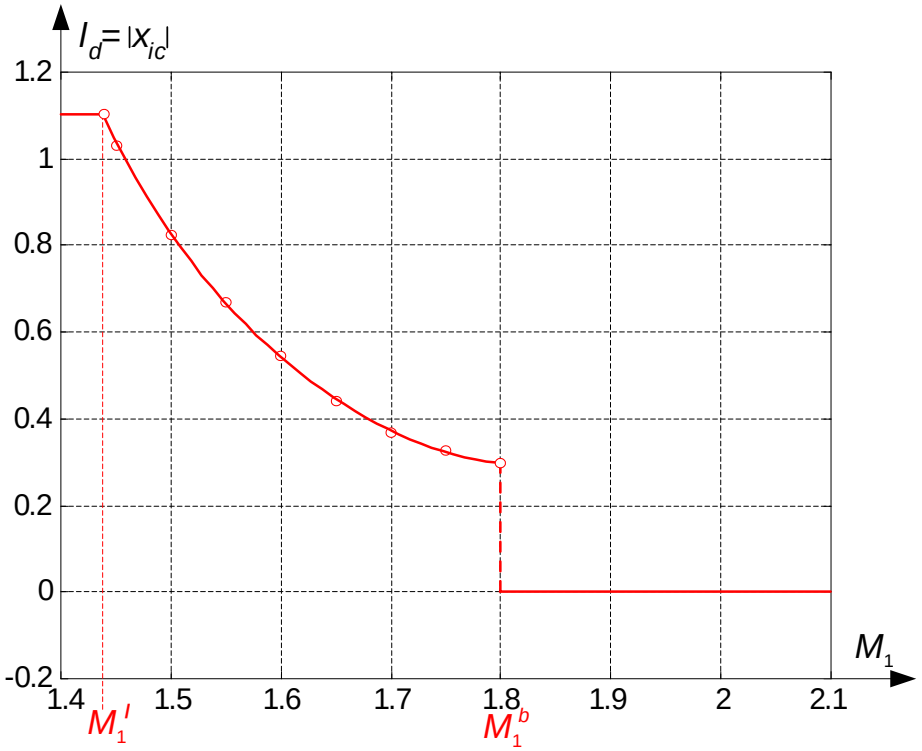

FIG. 8. Inlet's complementary control law (intake's cowl displacement)

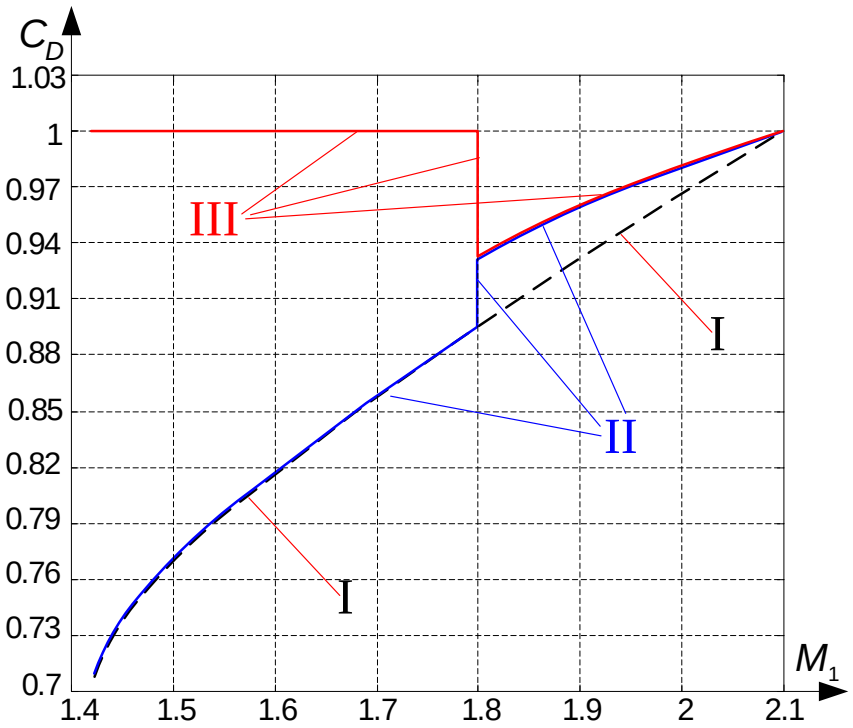

FIG. 9. Inlet's flow rate characteristics maps for different control laws

the cowl remains extended, the new born second oblique shock-wave has a small β_2 – angle and it would be developed inside the intake, which is forbidden (because of reflected shock-waves appearance and flow's speed and pressure fields distortion). Consequently, in order to make possible the main law operation, the cowl must be totally retracted when M_1^b – value is reached, so the point D/ in Fig. 7 regains its initial position D.

The complementary law for the intake's cowl displacement is graphically represented in Fig. 8; it has three important zones: a) the first zone, for subsonic and low supersonic airspeeds ($M_1 < M_1^{/}$), when the cowl is completely extended, b) the second (nonlinear) zone, between $M_1^{/}$ and M_1^b airspeeds, respectively c) the third high supersonic airspeeds zone ($M_1 > M_1^b$), when the cowl is completely retracted. At $M_1 = M_1^b$ the cowl must be sudden retracted.

As analytical expression, between $M_1^{/}$ and M_1^b the complementary control law has the form:

$$l_d(M_1) = 29.181M_1^4 - 195.823M_1^3 + 497.021M_1^2 - 566.728M_1 + 245.809. \quad (16)$$

The complementary law applying brings an improvement of the flow rate characteristics, especially for small airspeeds. The curve III in Fig. 9 corresponds to a simultaneously operating of the above-described control laws.

CONCLUSIONS

Supersonic inlets are built in a variety of shapes and sizes which are usually dictated both by the speed of the aircraft and by the position of the inlet on aircraft's airframe.

A plan supersonic inlet with a single mobile ramp, operating on a supersonic aircraft (flying at a Mach number M_H =2.5), mounted below its wing, was studied in this paper. For such a flying Mach number, the airflow in front of the inlet corresponds to a Mach number around 2.1, which was considered the nominal airspeed input, used for the inlet's design.

Inlet's architecture was established using an optimization criterion: the maximization of inlet's efficiency, which means the maximization of overall inlet's total pressure drop σ_i^*. Main geometric elements of the inlet are: centerbody's (spike's) flare angles (θ_1 and θ_2), centerbody's panels' lengths (l_1 and l_2), as well as cowl lip's position. All of these elements were determined for a hypothetical fixed geometry inlet, for a nominal frontal Mach number $M_1 = 2.1$.

Unlike the axially symmetrical inlets (which have conical-shape centerbodies and their control laws are based only on these centerbodies longitudinal displacement), plan (or rectangular) inlets have as control possibilities both spike or cowl longitudinal displacement and spike's second panel's rotation.

Since the studied inlet has a spike-shaped body (with a fixed panel and a hinged mobile panel), its main control law (with respect to the flight regime - altitude and speed), was determined as second panel's angle versus Mach number in front of the inlet. Consequently, the inlet operates in two different situations: a) for $M_1 < 1.8$ the mobile panel is extending the fixed panel, so the inlet works as "1+1"-type; b) for $1.8 \le M_1 \le 2.1$, the inlet works as "2+1"-type and the control law $\theta_2 = \theta_2(M_1)$ means a non-linear dependence on M_1, developed between $(\theta_2)_{\min} = 4.2^\circ$ and $\theta_{2_{\max}} = \theta_{2_{opt}} = 12.22^\circ$.

Applying the main control law with respect to the flight regime, it assures a better inlet efficiency, but an improper flow rate co-efficient behavior, especially for small airspeed values. Consequently, a complementary control law was issued, in order to improve inlet's behavior at low Mach numbers (airspeeds in front of the inlet), concerning the inlet's cowl displacement with respect to the same Mach number M_1. The complementary law is also non-linear, but its applying grows the flow rate coefficient C_D for low supersonic airspeeds, lower than 1.8 Mach.

Both issued motion laws are determined with respect to the flight regime (flight altitude and airspeed, given by the Mach number in front of the inlet). Although, the inlet is sensitive to engine's speed changes too; in fact, engine's regime affects the position of the normal shock-wave in front of the intake [6, 9,10], so other control laws, with respect to aircraft engine's regime, could be issued, but using the same mobile elements (such as intake's cowl).

The paper could be extended with the issuing of such control laws, as well as with control systems architecture studies.

REFERENCES

[1] Abraham, R. H. *Complex dynamical systems*. Aerial Press, Santa Cruz, California, 1986;
[2] Aron, I., Tudosie, A., Hydromechanical System For The Supersonic Air Inlet's Channel's Section Control, pp. 266-269, *Proceedings of the International Conference on Applied and Theoretical Electricity*, Craiova, 2000;
[3] Lungu, R. *Flight apparatus automation*. Publisher Universitaria, Craiova, 2000;
[4] Mattingly, J. D. *Elements of gas turbine propulsion*. McGraw-Hill, New York, 1996*;*
[5] Stevens, B.L., Lewis, E. *Aircraft control and simulation*, John Willey Inc. N. York, 1992;
[6] Pimsner, V. *Air-breathing jet engines. Processes and characteristics*. Didactical and Pedagogical Publisher, Bucharest, 1984;
[7] Pimsner, V., Berbente, C. and others, *Flows in turbomachinery*, Tehnica Publishing Bucharest, 1986, ISBN 973-165-4-17;
[8] Ran, H. and Mavris, D. Preliminary Design of a 2D Supersonic Inlet to Maximize Total Pressure Recovery, pp. 1-11, *Proceedings of AIAA 5th Aviation, Technology, Integration, and Operations Conference (ATIO)*, Arlington, Virginia, USA, 26 - 28 Sept. 2005;
[9] Rotaru, C., Sprintu, I. State Variable Modeling of the Integrated Engine and Aircraft Dynamics, pp. 889-898, *Proceedings of ICNPAA 2014 (10th International Conference On Mathematical Problems In Engineering, Aerospace And Sciences)*, Narvik, Norway, 15-18 July, 2014.
[10] Seddon, J. and Goldsmith, E. L. *Intake Aerodynamics*, 2nd edition, AIAA Education Series, 1999.
[11] Tudosie, A. Shock-waves within plan supersonic inlets, pp. 111-115, *Proceedings of XVth Session of scientific papers*, Naval Academy, Constanta, 5-7 th Nov. 1997;

[12] Tudosie, A. Plan supersonic intake with reflected shock-wave, pp. 229-234, *Proceedings of International Conference on Applied and Theoretical Electricity ICATE'98*, Craiova, 4-5th June 1998.
[13] Tudosie, A., Dragan, A. Rectangular supersonic air inlet with movable ramp, pp. 453-458, *Proceedings of International Conference on Applied and Theoretical Electricity ICATE 2002*, Craiova, 17-18th Oct. 2002.
[14] Tudosie, A. *Aerospace propulsion systems automation*, Inprint of University of Craiova, 2005.